

Observation of large $h/2e$ and $h/4e$ oscillations in a proximity dc superconducting quantum interference device

J. Wei, P. Cadden-Zimansky and V. Chandrasekhar

Department of Physics and Astronomy, Northwestern University, Evanston, IL 60208, USA

We have measured the magnetoresistance of a dc superconducting quantum interference device in the form of an interrupted mesoscopic normal-metal loop in contact with two superconducting electrodes. Below the transition temperature of the superconducting electrodes, large $h/2e$ periodic magnetoresistance oscillations are observed. By adding a small dc bias to the ac measurement current, $h/4e$ oscillations can be produced. Lowering the temperature further leads to even larger oscillations, and eventually to sharp switching from the superconducting state to the normal state. This flux-dependent resistance could be utilized to make highly sensitive flux detector.

Superconducting Quantum Interference Devices (SQUIDs) are ideal for detecting extremely small changes in magnetic fields and have undergone extensive development and evolution for over 40 years.^{1,2} The dc SQUID consists of two Josephson junctions connected in parallel. When biased above its critical current, the dc voltage across the SQUID is modulated by a magnetic flux. For proper operation, additional resistive shunts across the junctions are usually required to remove the hysteretic behavior of the device. The Nyquist noise of these resistive shunts limits the sensitivity of the SQUID. Recently, with advances in nanofabrication techniques, it has become possible to fabricate a mesoscopic SQUID with the Josephson junctions composed of normal metal sections with lengths shorter than the normal metal coherence length ξ_N . The use of normal metal junctions enables the SQUID to be intrinsically shunted, allowing for the possibility of increased sensitivity. Additionally, it may eliminate the low frequency noise due to weakly trapped charges in the Josephson barrier, which is a major obstacle for realizing long-lived quantum states in SQUIDs.³ Since the resistance of the superconducting-normal-superconducting (SNS) junction changes with temperature due to the superconducting proximity effect, the properties of this proximity dc SQUID are quite different from traditional SQUIDs which use junctions made of thin insulating barriers. In this work, we investigate the behavior of such a proximity dc SQUID and find unusually large magnetoresistance oscillations with both $h/2e$ and $h/4e$ periods. In addition, at low temperatures the SQUID undergoes flux-dependent switching from the superconducting to the normal state, which may be useful for applications.

The inset of Fig. 1 shows SEM images of two different devices. The geometry is that of an interrupted normal-metal Au loop in contact with two superconducting Al electrodes. The loop is broken into two arms, which each serve as a Josephson junction between the superconducting electrodes. The separation between the two arms is 100 nm for the upper device in the inset, and 40 nm for the lower one (the separation is not clear in this SEM image due to the overlap of the Al and Au layers). This separation is smaller than the typical superconducting coherence length ξ_S for Al.⁴ The width of the normal metal

arms of the loop is 90 nm and the length of each arm is approximately $1 \mu\text{m}$. As shown by the schematic in Fig. 1, the superconducting Al electrodes extend for several micrometers on each side before overlapping with Au leads used to make four-probe measurements. Conventional bilayer (PMMA/MMA) e -beam lithography was used to pattern the devices on oxidized Si substrates. The 50 nm thick Au was deposited first in a thermal evaporator with base pressure 3×10^{-7} Torr at a rate of 0.6 nm/sec. After further patterning, an *in situ* Ar⁺ plasma etch was performed just prior to the deposition of the 80 nm thick Al wires to ensure transparent interfaces. After the fabrication of the Al wires the devices were immediately loaded into a dilution refrigerator with base temperature lower than 20 mK. Differential resistance measurements were performed with conventional ac bridge and lock-in techniques using measurement currents of 20 -100 nA.

The resistance for each of the two devices as a function of temperature is shown in Fig. 1. Since both devices yielded similar results, in what follows we will focus our discussion on the upper one. As the temperature is decreased there is a sharp drop in the resistance at 1.2 K, corresponding to the transition temperature of the Al electrodes between the voltages probes. The remaining resistance of about 5Ω just below this transition temperature is the resistance of the Au loop. Due to the proximity effect caused by the superconducting Al electrodes, this resistance drops as the temperature is further decreased, eventually reaching zero at 0.7 K. The pronounced nature of the proximity effect just below 1.2 K is an indication of highly transparent N-S interfaces.⁵ Below 0.7 K, where the resistance is zero, the critical current of the loop is measured by applying a dc bias current in addition to the ac measurement current. As shown in Fig. 1, the critical current continues to increase with decreasing temperature and does not saturate. However, below 0.45 K the critical current displays hysteresis depending on the direction of the current sweep, as has been reported in other experiments on similar structures.^{6,7} Whether the hysteresis is due to thermal effects or intrinsic damping caused by the normal metal has not been determined.⁷

From the normal resistance of the loop, and the resistance of a simultaneously fabricated long normal wire

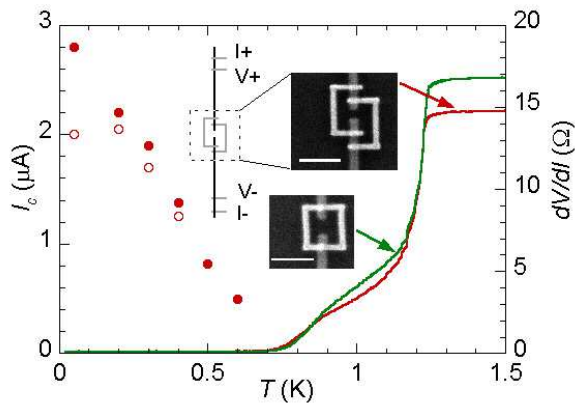


FIG. 1: (Color online) Right scale: Resistance as a function of temperature for the two proximity SQUIDs shown in the inset; the data are taken using an ac measurement current of $I_{\text{meas}} = 100$ nA. Left scale: Temperature dependence of the critical current derived from differential resistance vs. bias current measurements for the upper one of the two devices. The ac measurement current is 100 nA above 450 mK and 20 nA below 450 mK. Below 450 mK, the retrapping currents (open circles) were clearly different from the switching currents (solid circles), indicating hysteresis. Inset: Schematic of the four-probe measurement configuration and SEM images of the two devices. The arms of the loops (brighter wires) are made of Au and the electrodes extending out of the top and bottom (darker wires) are made of Al. The size bar in both images is 500 nm.

sample on the same chip, the resistance per square R_{\square} of the Au film is found to be 0.8Ω . From this we calculate an elastic mean free path $l = 21$ nm and a diffusion constant $D = 97$ cm²/sec. Since the length of each normal metal arm L is approximately $1 \mu\text{m}$, the corresponding Thouless energy, $\epsilon_c = \hbar D/L^2$, is $6.6 \mu\text{eV}$ and Thouless temperature, $T_{\text{Th}} = \epsilon_c/k_B$, is 77 mK. For SNS proximity junctions, theory predicts that in the long junction limit, i.e., $L \gg \sqrt{\hbar D/\Delta}$ or $\Delta/\epsilon_c \gg 1$, the critical current increases exponentially with decreasing T , and as T approaches T_{Th} the ratio $eR_N I_c/\epsilon_c$ should saturate at 10.82 .⁸ However, for our dc SQUID with two junctions in parallel, $\Delta/\epsilon_c \sim 26$, but the ratio $eR_N I_c/\epsilon_c$ at 50 mK is about 2.3 , a factor of 5 smaller than expected. The discrepancy may be due to the theoretical assumption of perfect interfaces, or due to the presence of thermally activated phase slipping in 1-D proximity-coupled normal wire at low temperatures,⁹ which can lead to premature switching. In addition, since the length of the normal metal arm is comparable to the phase coherence length, the suppression of critical current could also be attributed to various dephasing effects¹⁰.

Figure 2 shows the differential resistance as a function of magnetic flux through the loop at different dc bias currents (I_{bias}). The data is taken at 0.8 K where the normal-metal loop is in the proximity regime. At zero dc bias, the magnetoresistance shows large oscillations with a period corresponding to one superconducting flux

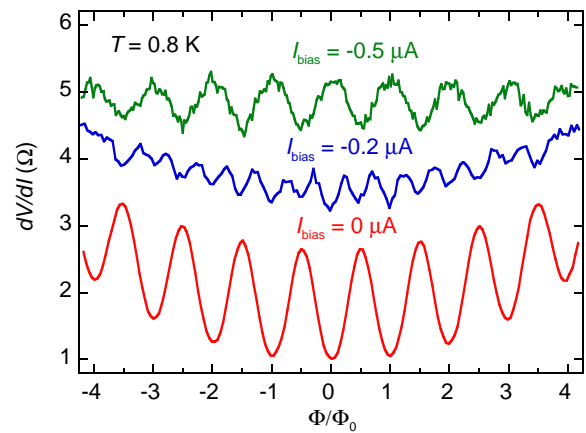


FIG. 2: (Color online) Magnetoresistance of the top loop in Fig. 1 at 800 mK for different dc bias currents. The applied flux is measured in units of superconducting flux quanta, $\Phi_0 = h/2e$, corresponding to a field of 47 G for this device. With increasing bias current, the oscillation evolves from $h/2e$ periodic oscillations to $h/4e$ periodic oscillations and then to inverted $h/2e$ oscillations.

quantum $\Phi_0 = h/2e$ for the enclosed area of the loop. The amplitude of the oscillation is about 1.8Ω , more than 30% of the normal state resistance. Similar $h/2e$ oscillations have been reported previously, and were interpreted as the interference of long-range coherent quasiparticles.^{5,11} However, in this earlier work the proximity effect was thought to be determined by T_{Th} and the amplitude of the oscillations by T_{Th}/T .^{12,13} Although T_{Th} of our devices is similar to that of these earlier devices, the amplitude of the observed oscillations is much larger and the Josephson coupling begins to dominate at a much higher temperature than T_{Th} .

When a dc bias $I_{\text{bias}} = -0.2 \mu\text{A}$ is added to the ac measurement current, oscillations in the flux with half the period, i.e., $h/4e$, are clearly present (see Fig. 2). The $h/4e$ oscillations here follow a similar quadratic envelope as that of the $h/2e$ oscillations, and also have their minima at integer flux quanta, although the amplitude of the oscillations is smaller. When a higher dc bias $I_{\text{bias}} = -0.5 \mu\text{A}$ is applied, the $h/2e$ oscillations are recovered with a π phase shift compared to the $h/2e$ oscillations at zero-bias current. The differential resistance at this bias is close to the normal-state resistance and the background magnetoresistance is flat.

To demonstrate how the $h/4e$ oscillations are produced, the differential resistance as a function of bias current for different values of magnetic flux through the loop is measured (Fig. 3(a)).¹⁴ At $I_{\text{bias}} = -0.53 \mu\text{A}$ (marked by the middle vertical arrow) the differential resistance at zero and one flux quantum is close to that at a half-flux quantum, and the differential resistance at one-quarter and three-quarter flux quanta are both higher than that at a half-flux quantum. Thus the magnetoresistance at $I_{\text{bias}} = -0.53 \mu\text{A}$ oscillates with half the usual period,

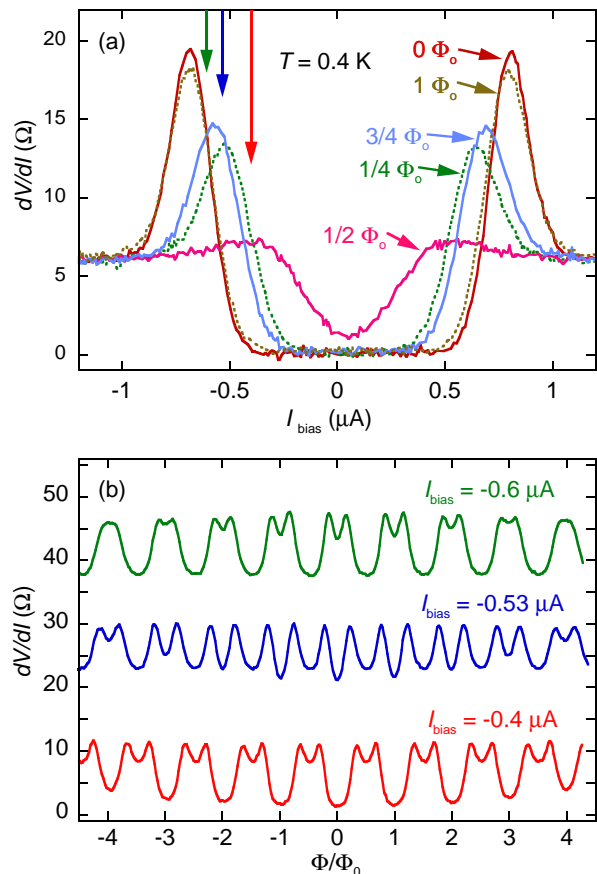


FIG. 3: (Color online) (a) dc bias current dependence of the differential resistance at 0.4 K for different applied magnetic fluxes. The three vertical arrows indicate where two curves cross each other. (b) From the bottom up, the differential magnetoresistance at -0.4 , -0.53 , and -0.6 μA respectively, showing the evolution to $h/4e$ oscillations. The two upper curves are offset by 15 Ω and 30 Ω respectively for clarity.

as shown in Fig. 3(b). Note that here the amplitude of $h/4e$ oscillation can be larger than the normal-state resistance since the differential resistance is determined by the slope of the I-V curve. At a slightly lower bias current, $I_{\text{bias}} = -0.4$ μA , the $h/4e$ oscillation starts to appear on top of the $h/2e$ oscillation. At a slightly higher bias current, $I_{\text{bias}} = -0.6$ μA , inverted $h/2e$ oscillations replace the $h/2e$ oscillations.

Oscillations with $h/4e$ period have been reported before in mesoscopic SNS structures¹¹ and in superconducting cylinders.¹⁵ However, in these cases no dc bias was intentionally applied, and the amplitude of the $h/4e$ oscillations was orders of magnitude smaller. The $h/4e$ oscillations were ascribed to the interplay between multiple Andreev reflections and interference in the first case,¹¹ and to an odd number of π -junctions in the second case.¹⁵ The observation of $h/4e$ oscillations in our own device leads us to another possible explanation for the oscillations seen previously: as the two arms of a loop are not perfectly symmetrical, some finite dc voltage can be in-

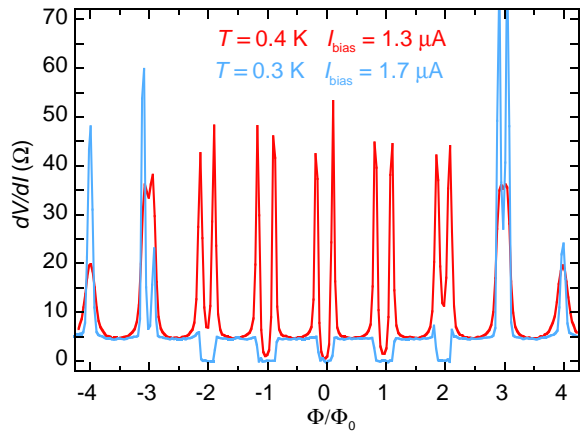


FIG. 4: (Color online) Differential magnetoresistance at 0.3 K and 0.4 K with dc bias current set close to the differential resistance peak. The periodic peaks in the magnetoresistance are mostly absent at 0.3 K, likely due to the peak width at this temperature being smaller than the measurement current.

duced due to rectification of the ac measurement current and ac noise^{16,17,18}. This dc voltage may push the device into a biased regime where $h/4e$ oscillations can be observed as in Fig. 3.

When the temperature is further lowered, Figure 4 shows that the differential magnetoresistance peaks become quite sharp, with peak values more than 10 times the normal state resistance. Although the $h/2e$ period persists, the shape of the oscillations is no longer symmetric. For $T = 0.3$ K most of the peaks disappear as the oscillations evolve to become peakless switching from the normal resistance state to the zero resistance state. The evolution from sharp peaks to peakless switching was also found for the bias current dependence of the differential resistance as the temperature is lowered. In both cases, the disappearance of the peaks is likely due to the amplitude of the ac measurement current being larger than the width of the differential resistance peaks at low temperatures. For applications this strong dependence of the differential resistance on the flux may be useful for sensing small changes in the flux.

In summary, we have measured a dc SNS SQUID in the form of an interrupted mesoscopic normal-metal loop in contact with two superconducting electrodes. Unusually large $h/2e$ oscillations, $h/4e$ oscillations, and $h/2e$ oscillation with a π phase shift were found. The $h/4e$ oscillation can be readily explained by considering the bias current dependence of the differential resistance. At lower temperatures these oscillations show high, flux-dependent differential resistance peaks which evolve to sharp, peakless switching between the normal and superconducting states. This rapid change of differential resistance may be useful for flux sensitive measurements.

This work was funded by the NSF through grant DMR-0604601.

-
- ¹ A. Barone and G. Paternò, *Physics and Applications of the Josephson Effect* (John Wiley, 1982).
 - ² J. Clarke and A. Braginski, *The SQUID handbook* (Weinheim : Wiley-VCH, 2004).
 - ³ M. Mück, M. Korn, C. G. A. Mugford, J. B. Kycia, and J. Clarke, *Appl. Phys. Lett.* **86**, 012510 (2005).
 - ⁴ P. Cadden-Zimansky and V. Chandrasekhar, *Phys. Rev. Lett.* **97**, 237003 (2006).
 - ⁵ H. Courtois, P. Gandit, D. Mailly, and B. Pannetier, *Phys. Rev. Lett.* **76**, 130 (1996).
 - ⁶ C. Hoffmann, F. Lefloch, M. Sanquer, and B. Pannetier, *Phys. Rev. B* **70**, 180503 (2004).
 - ⁷ L. Angers, F. Chiodi, J. C. Cuevas, G. Montambaux, M. Ferrier, S. Gueron, and H. Bouchiat, arXiv:0708.0205.
 - ⁸ P. Dubos, H. Courtois, B. Pannetier, F. K. Wilhelm, A. D. Zaikin, and G. Schön, *Phys. Rev. B* **63**, 064502 (2001).
 - ⁹ M. Tinkham, *Introduction to Superconductivity* (McGraw Hill, 1996).
 - ¹⁰ D. S. Golubev, A. D. Zaikin, *Physica E* **40**, 32 (2007).
 - ¹¹ V. T. Petrashov, V. N. Antonov, P. Delsing, and R. Claeson, *Phys. Rev. Lett.* **70**, 347 (1993). V. Petrashov, V. Antonov, P. Delsing, and T. Claeson, *Physica B* **194-196**, 1105 (1994).
 - ¹² H. Courtois, P. Gandit, B. Pannetier, and D. Mailly, *Superlatt. Microstruc.* **25**, 721 (1999).
 - ¹³ A. A. Golubov, F. K. Wilhelm, and A. D. Zaikin, *Phys. Rev. B* **55**, 1123 (1997).
 - ¹⁴ Data in this figure were measured after thermal cycling to room temperature, which leads to reduced critical currents due to degraded S-N interfaces.
 - ¹⁵ Y. Zadorozhny and Y. Liu, *Europhys. Lett.* **55**, 712 (2001).
 - ¹⁶ S. V. Dubonos, V. I. Kuznetsov, I. N. Zhilyaev, A. V. Nikulov, and A. A. Firsov, *JETP Lett.* **77**, 371 (2003).
 - ¹⁷ J. Berger, *Phys. Rev. B* **70**, 024524 (2004).
 - ¹⁸ S. Weiss, D. Koelle, J. Müller, R. Gross, and K. Barthel, *Europhys. Lett.* **51**, 499 (2000).